On the Accurate Finite Element Solution of a Class of Fourth Order Eigenvalue Problems

B.M. Brown* E.B. Davies† P.K. Jimack‡ M.D. Mihajlović*

Abstract

This paper is concerned with the accurate numerical approximation of the spectral properties of the biharmonic operator on various domains in two dimensions. A number of analytic results concerning the eigenfunctions of this operator are summarized and their implications for numerical approximation are discussed. In particular, the asymptotic behaviour of the first eigenfunction is studied since it is known that this has an unbounded number of oscillations when approaching certain types of corner on domain boundaries. Recent computational results of Bjørstad and Tjøstheim [4], using a highly accurate spectral Legendre-Galerkin method, have demonstrated that a number of these sign changes may be accurately computed on a square domain *provided* sufficient care is taken with the numerical method. We demonstrate that similar accuracy is also achieved using an unstructured finite element solver which may be applied to problems on domains with arbitrary geometries. A number of results obtained from this mixed finite element approach are then presented for a variety of domains. These include a family of circular sector regions, for which the oscillatory behaviour is studied as a function of the internal angle, and another family of (symmetric and non-convex) domains, for which the parity of the least eigenfunction is investigated. The paper not only verifies existing asymptotic theory, but also allows us to make a new conjecture concerning the eigenfunctions of the biharmonic operator.

1 Introduction

In recent years there has been growing interest in the spectral theory of higher order elliptic operators. However, in contrast to the well-understood theory for second order operators, the higher order theory can be quite different and is certainly less well developed. The recent survey article [14] contains an account of many of the key results. The purpose of this paper is to explore, using reliable and accurate numerical techniques, some of the properties of the eigenfunctions of the biharmonic operator on domains in $\Re^2$. In particular we investigate the existence of so-called *nodal lines* in the neighbourhood of certain corners of the domain and also how the parity of these eigenfunctions may change with domain geometry. As will become clear from the quantitative description of these problems below this is a demanding computational task since very high numerical accuracy is required in order to resolve the phenomena under investigation.

The biharmonic eigenvalue problem typically comes in two different forms: the clamped plate eigenproblem

$$\Delta^2 u = \lambda u \ , \tag{1}$$

*Department of Computer Science, Cardiff University of Wales, Cardiff CF2 3XF, Wales, UK.
†Department of Mathematics, King's College London, Strand, London WC2R 2LS, UK.
‡School of Computer Studies, University of Leeds, Leeds LS2 9JT, UK.

and the buckling plate eigenproblem

$$\Delta^2 u = \lambda \Delta u \ , \tag{2}$$

each on a domain $\Omega \subset \Re^2$ subject to appropriate conditions on the boundary $\partial\Omega$. Throughout this paper we shall consider only the zero Dirichlet conditions

$$u = \frac{\partial u}{\partial n} = 0 \quad \forall x \in \partial\Omega. \tag{3}$$

In the remainder of this introductory section we describe details of the specific problems that are to be considered. Section 2 then contains an outline and justification of the numerical techniques, based upon the use of conforming C^0 finite elements, that are used to undertake these investigations. This is followed in Sections 3 and 4 respectively by our findings concerning oscillations of the eigenfunctions in the neighbourhood of corners of the domain and the dependence of the parity of the eigenfunctions on the domain geometry. The paper concludes with a brief discussion of our results along with a consideration of the issues associated with the validation of numerical simulations such as these, including mesh convergence and the use of rigorous enclosure techniques.

1.1 Oscillatory properties of eigenfunctions

For each of the two problems (1) and (2) it is shown in [6],[12] that in the neighbourhood of a corner of $\partial\Omega$ with sufficiently small internal angle θ any eigenfunction changes sign an infinite number of times. Moreover the ratio of the distance from the corner, along its bisector, of consecutive zeros of the eigenfunction tends to a limit which is dependent upon θ. It transpires that this ratio is an increasing function of θ and is such that the oscillations cease to be present when the internal angle exceeds some critical value θ_c.

These results are special cases of more general theorems concerning higher order elliptic operators in greater than one dimension [18]. Their derivation is based upon an asymptotic expansion of the eigenfunction, u, centred at, and in a neighbourhood of, the corner. The leading term of such an expansion as one approaches the corner along the bisector of the angle (which we always do) is of the form cr^p, where r is the distance from the corner, and p is a solution of the transcendental equation

$$p + 1 + \frac{\sin\left((p+1)\theta\right)}{\sin\theta} = 0. \tag{4}$$

Assuming that the coefficient c is non-zero the relevant solution is the one with smallest real part. From this equation, which has only real solutions for $\theta > \theta_c = 0.8128\pi = 146°30'$, it may be concluded that when the internal angle is greater than θ_c the eigenfunction has no sign changes near the corner. Conversely as $\theta \to 0$ both the real and imaginary parts of the exponent of the leading term in the asymptotic expansion grow unboundedly, implying that the eigenfunction oscillates with high frequency but is damped out quickly for small θ. Moreover, when we let s_n be the distance along the bisector from the corner to the n^{th} zero of u, where n increases with decreasing distance from the corner, then it follows immediately from the asymptotic expression that

$$\frac{s_n}{s_{n+1}} \sim e^{\pi/\beta} \quad \text{as } n \to \infty, \tag{5}$$

where $p = \alpha + i\beta$ is the solution of (4) with smallest real part. Furthermore, when r_n is the distance along the bisector to the n^{th} extremum of u and t_n is the magnitude of this extremum, it may also be shown that

$$\frac{r_n}{r_{n+1}} \sim \frac{s_n}{s_{n+1}} \qquad \text{and} \qquad \frac{t_n}{t_{n+1}} \sim \left(\frac{s_n}{s_{n+1}}\right)^{\alpha} \tag{6}$$

as $n \to \infty$. The first goal of this research is to verify this behaviour for a sequence of domains which take the form of sectors of a circle with increasing arc length. In view of the above discussion and the data in Table 1 below it is clear that such a verification will require very high accuracy from the numerical methods used. This table presents the solutions $p = \alpha + i\beta$ of (4) as a function of θ, as well as the ratios $e^{\pi/\beta}$ and $e^{\alpha\pi/\beta}$ which appear in (5) and (6). These solutions of (4) are obtained by Newton's method with double precision arithmetic.

θ	10°	20°	30°	40°	50°	60°	70°
$\alpha = \Re e(p)$	25.141144	13.079480	9.062965	7.057831	5.857356	5.059329	4.491404
$\beta = \Im m(p)$	12.864086	6.384388	4.202867	3.095366	2.416840	1.952050	1.608491
$e^{\pi/\beta}$	1.27662	1.63571	2.11169	2.75918	3.66884	4.99972	7.05073
$e^{\alpha\pi/\beta}$	463.97239	623.95258	875.20459	1291.07923	2026.03589	3437.12115	6452.99420

θ	80°	90°	100°	110°	120°	130°	140°
$\alpha = \Re e(p)$	4.067435	3.739593	3.479215	3.268096	3.094139	2.949023	2.826869
$\beta = \Im m(p)$	1.339586	1.119024	0.930373	0.762118	0.604585	0.446356	0.261695
$e^{\pi/\beta}$	10.43532	16.56743	29.27404	61.69387	180.5992	1139.464	163533.23
$e^{\alpha\pi/\beta}$	13890.112	36267.559	126534.61	709058.99	9607097.6	1033431725	$0.5472 \cdot 10^{15}$

Table 1: The solutions of (4) as a function of the angle θ. The ratios $e^{\pi/\beta}$ and $e^{\alpha\pi/\beta}$ are also given.

1.2 Parity of eigenfunctions for non-convex domains

Our other main goal is to investigate the dependence of the parity of the eigenfunctions of problems (1) and (2) on the geometry of Ω. Given a domain $\Omega \subset \Re^2$ which is symmetric about some line (which, without loss of generality, we will choose to be the y-axis), it is known that the least eigenfunction of the *Laplace* operator, subject to zero Dirichlet boundary conditions, is always positive and of multiplicity one [13]. Symmetry arguments now force it to be an even function of x. No equivalent result holds for the biharmonic operator. Indeed, it is the purpose of this work to demonstrate numerically that no such result holds for problems of the form (1) and (2) in arbitrary symmetric domains Ω. This is achieved in Section 4 by considering a family of non-convex domains whose boundary is defined by the closed curves

$$y = \pm(c + x^2 - x^4) \tag{7}$$

for $c > 0$ (see figure 1 below). Domain monotonicity arguments [13] imply that the eigenvalues of the biharmonic operator increase as $c \to 0$ and converge to the eigenvalues of the same operator on the region associated with $c = 0$. This region is disconnected and its eigenvalues have multiplicity two. Variational considerations now show that for small enough $c > 0$ the low-lying eigenvalues occur in pairs, one associated with an even eigenfunction and the other associated with an odd eigenfunction. However in the biharmonic case one cannot say which of these is the smaller on purely variational grounds. Indeed by monitoring the smallest two eigenvalues of (1) or (2) as functions of c, it may be observed that their paths cross on more than one occasion as $c \to 0$. Furthermore it is apparent that one of these eigenvalues corresponds to an even eigenfunction while the other corresponds to an odd one, and consequently we observe that the parity of the least eigenfunction is not fixed as a function of c. We again remark on the need for very high accuracy in our computational algorithms; this time in order to identify values of c for which the eigenvalue paths cross.

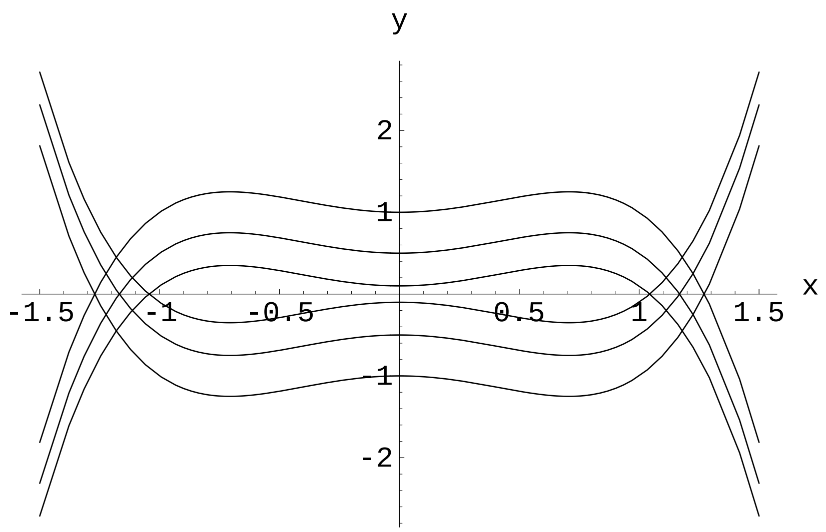

Figure 1: The dumb-bell shape domain for $c = 1,\ c = 0.5,\ c = 0.1$

2 Numerical method

Given the above discussion, it is clear that our discretization scheme must be able to accommodate quite general domain geometries. For this reason we choose a numerical scheme which is based upon the use of conforming C^0 Lagrange finite elements (see [21],[25] for example) on some triangulation of the domain Ω. The particular method that we use is based on that of Ciarlet and Raviart in [11].

Let $H^1(\Omega)$ represent the usual Sobolev space of $L^2(\Omega)$ functions whose first partial derivatives are in $L^2(\Omega)$, and

$$H_0^1(\Omega) = \left\{ \psi \in H^1(\Omega) : \psi|_{\partial\Omega} = \left.\frac{\partial \psi}{\partial n}\right|_{\partial\Omega} = 0 \right\}.$$

Consider a family of regular and quasi-uniform triangulations, $\mathcal{T}^h$ (where h is the diameter of the largest triangle), of the domain Ω (see, for example, Ciarlet [10]), then we may define the space

$$\mathcal{S}_m^h = \{ p \in C^0(\bar{\Omega}) \,:\, p|_T \in P_m(T),\ \forall T \in \mathcal{T}^h \},$$

where $P_m(T)$ is the space of polynomials of degree at most m over triangle T. From this we may define the following finite-dimensional subspaces of $H^1(\Omega)$: $V^h = \mathcal{S}_m^h$ and $W^h = \mathcal{S}_m^h \cap H_0^1(\Omega)$. Then the Ciarlet–Raviart mixed finite element method approximates the solution u of (1) by the component u^h of the solution $\{v^h, u^h\} \in V^h \times W^h$ to the following problem.

Problem 2.1 *Find* $\{v^h, u^h\} \in V^h \times W^h$ *such that*

$$\begin{aligned} \int_\Omega v^h w_1 \, d\Omega + \int_\Omega \nabla u^h \cdot \nabla w_1 \, d\Omega &= 0 \qquad \forall w_1 \in V^h, \\ \int_\Omega \nabla v^h \cdot \nabla w_2 \, d\Omega &= -\lambda \int_\Omega u^h w_2 \, d\Omega \quad \forall w_2 \in W^h. \end{aligned}$$

In this work we choose $m = 3$, i.e. piecewise cubic approximation, since such a discretization is known to satisfy the Brezzi stability condition, [7], [20] and has the following asymptotic error property ([11]):

$$\|u - u^h\|_{H^1(\Omega)} + \|\Delta u - v^h\|_{L_2(\Omega)} \leq c \|u\|_{H^5(\Omega)} h^2\ , \tag{8}$$

provided the solution u is sufficiently smooth. Hence the trial functions v^h and u^h in Problem 2.1 may be expressed as

$$v^h = \sum_{j=1}^{n_i+n_d} v_j \phi_j \qquad \text{and} \qquad u^h = \sum_{j=1}^{n_i} u_j \phi_j, \tag{9}$$

where the ϕ_j's are the usual piecewise cubic Lagrange basis functions on $\mathcal{T}^h$ (see [21],[25] for example), and n_i and n_d are the number of nodes in the interior of Ω and on its Dirichlet boundary respectively. (We also use the convention that the interior nodes are numbered prior to those on the Dirichlet boundary.) This discretization leads to the following matrix problem

$$\begin{bmatrix} M & K^t \\ K & O \end{bmatrix} \begin{bmatrix} \underline{v} \\ \underline{u} \end{bmatrix} = -\lambda \begin{bmatrix} \underline{0} \\ \hat{M}\underline{u} \end{bmatrix}, \tag{10}$$

where $M \in \Re^{(n_i+n_d)\times(n_i+n_d)}$, $\hat{M} \in \Re^{n_i \times n_i}$ is a principal submatrix of M, $K \in \Re^{n_i \times (n_i+n_d)}$ and K^t is the transpose of K. The specific entries of these matrices are given by

$$\begin{aligned} K_{ij} &= \int_\Omega \nabla\phi_i \cdot \nabla\phi_j \; d\Omega, \\ M_{ij} &= \int_\Omega \phi_i \phi_j \; d\Omega, \end{aligned}$$

and the vectors $\underline{v} \in \Re^{n_i+n_d}$ and $\underline{u} \in \Re^{n_i}$ denote the coefficients of v^h and u^h respectively in (9).

It may be observed that $\underline{u}$ and λ in (10) are generalized eigenvectors and eigenvalues respectively for the corresponding Schur complement problem:

$$KM^{-1}K^t\underline{u} = \lambda \hat{M}\underline{u}. \tag{11}$$

In this paper we are typically interested in approximating the smallest eigenvalues of this problem and so make use of straightforward inverse iteration (as described in [15] for example). Since the Schur complement matrix $KM^{-1}K^t$ is dense, whereas the matrix on the left-hand side of (10) is sparse, it is convenient to apply the inverse iteration to the latter system. This yields the following matrix equation at the $(n+1)^{th}$ inverse iteration:

$$\begin{bmatrix} M & K^t \\ K & O \end{bmatrix} \begin{bmatrix} \underline{v}^{n+1} \\ \underline{u}^{n+1} \end{bmatrix} = \begin{bmatrix} \underline{0} \\ -\hat{M}\underline{u}^n \end{bmatrix}. \tag{12}$$

When approximating the second smallest eigenpair, as in Section 4 for example, this iteration is slightly modified by subtracting out the component of the smallest eigenvector from $\underline{u}^{n+1}$ at each iteration.

We solve the systems (12) using a direct sparse method based upon an initial block reduction followed by a sparse Cholesky factorization of symmetric positive definite sub-blocks as described in [8]. This permits re-use of the factorizations for the second and subsequent solves, which ensures that the cost of these is significantly less than that of the initial solution of (12). An additional advantage of a direct, rather than an iterative, method such as this is that it is possible to obtain highly accurate solutions: something that is required in both Sections 3 and 4 below. To demonstrate the accuracy of this approach (both the discretization and the direct solution), we now present some typical numerical computations for a biharmonic eigenvalue problem which has been considered in some detail elsewhere, [4],[8].

Recall from Subsection 1.1 that in the neighbourhood of a corner with a sufficiently small internal angle, the eigenfunctions for both problems (1) and (2) are known to change sign at an infinite number of points. In particular, when the internal angle $\theta = \pi/2$ the solution of (4) with smallest real part is $3.739593284 + 1.1190248i$ (see Table 1). It then follows from (5) and (6) that the asymptotic ratio of distances along the bisector of consecutive zeros and extremal points of the eigenfunctions should both tend to 16.567428 as $n \to \infty$. Also from (6) we see that the ratios between the magnitudes of consecutive extrema along the bisector tends to 36267.550 as $n \to \infty$. In recent years many authors have tried to verify numerically these theoretical results using a variety of computational techniques (see, for example, [2],[9],[16],[24]). Since the oscillatory features occur very close to the corners and are damped out very quickly, most of these attempts have, due to discretization errors and numerical inaccuracy, failed to find more than one sign change. A notable exception to this is the recent paper of Bjørstad and Tjøstheim ([4]) in which the authors report five correct sign changes for the principal eigenfunction of problem (1) on the domain $(0,1) \times (0,1)$. This is achieved using a spectral Legendre–Galerkin method and by performing computations with quadruple precision arithmetic.

In Tables 2 to 5 we present some comparative numerical results of our own, obtained using the mixed finite element method described above on three different meshes. In addition we contrast in the last column of the tables 2, 4 and 5 the best results of Bjørstad and Tjøstheim reported in [4]. (This latter paper does not present results for the positions, s_n, of the zeros and so no comparisons are possible for these figures). It may clearly be seen that, for each of these meshes, we are also able to identify at least five sign changes for the principal eigenfunction of (1) on the unit square. These calculations have been undertaken using double precision arithmetic on one eighth of the domain, using symmetries at $x = 1/2$, $y = 1/2$ and $y = x$, and with heavy local refinement of the meshes near the corner ($h \approx 10^{-7}$ in the vicinity of the corner with a gradual transition to $h \approx 10^{-2}$ at the centre of the domain). The results are entirely consistent with the quadruple precision results presented in [4] and with the predicted asymptotic ratios (5) and (6). This leads us to have a reasonable degree of confidence in the underlying numerical procedure that we use for the investigations undertaken in the following two sections.

3 Eigenfunctions on a circular sector

The purpose of this section is to extend the numerical studies in [4],[8], which concern the behaviour of the principle eigenfunction of the biharmonic operator near the corners of a square domain, to the case of a general internal angle θ. This is achieved by considering a one parameter family of unit radius circular sector domains, Ω_θ, and applying to (1) the finite element discretization defined in Problem 2.1. Recall from Subsection 1.1 that the oscillatory behaviour of the eigenfunction, u, near to a corner depends upon the internal angle θ through the imaginary part of a solution of equation (4). In particular, there is a critical angle, θ_c, above which no oscillations are present. As usual all of our calculations are restricted to the behaviour of the eigenfunction on the bisector of the angle at the corner. In this study we examine in detail the behaviour of the oscillations in the principal eigenfunction as θ approaches $\theta_c = 0.8128\pi = 146°30'$, but we also present approximation of the eigenfunction for other values of the angle θ.

It has already been demonstrated in Section 2 that our finite element discretization scheme is capable of producing the accuracy that is required to resolve up to five sign changes when $\theta = \pi/2$, on the unit square, which is consistent with the best numerical results of which we are aware [4]. Clearly a key to obtaining results with this level of resolution near to the corner is the use of an appropriate triangulation $\mathcal{T}^h$. For the circular sector regions that we consider here we use a similar mesh generation strategy to that adopted for the one-eighth of the unit square in the previous section. This involves the creation of an unstructured mesh based upon polar coordinates centred at the vertex. When r is greater than some (very small) chosen value, ρ_1 say, the mesh is such that

	FE method			L–G method [4]
N	5575	22351	90028	5000
λ_1	1294.934809196	1294.934021432	1294.933981245	1294.933979592
s_1	0.042311747881	0.042310932855	0.042310963855	—
r_1	0.032634299694	0.032630435492	0.032629530244	0.032629472978
t_1	$-0.169815505603 \cdot 10^{-4}$	$-0.169795463221 \cdot 10^{-4}$	$-0.169791420686 \cdot 10^{-4}$	$-0.169791287981 \cdot 10^{-4}$
s_2	0.002553961304	0.002553862560	0.002553860600	—
r_2	0.001969665622	0.001969564641	0.001969500077	0.001969491936
t_2	$0.468412256179 \cdot 10^{-9}$	$0.468173039472 \cdot 10^{-9}$	$0.468161662361 \cdot 10^{-9}$	$0.468161006275 \cdot 10^{-9}$
s_3	0.000154151151	0.000154149893	0.000154149497	—
r_3	0.000118849965	0.000118881375	0.000118877347	0.000118877352
t_3	$-0.129136601165 \cdot 10^{-13}$	$-0.129088794006 \cdot 10^{-13}$	$-0.129085648295 \cdot 10^{-13}$	$-0.129085369432 \cdot 10^{-13}$
s_4	0.000009304900	0.000009304402	0.000009304373	—
r_4	0.000007177212	0.000007175502	0.000007175314	0.000007175365
t_4	$0.356091995705 \cdot 10^{-18}$	$0.355934162890 \cdot 10^{-18}$	$0.355925959506 \cdot 10^{-18}$	$0.355925258182 \cdot 10^{-18}$
s_5	0.000000561678	0.000000561628	0.000000561569	—
r_5	0.000000433175	0.000000432837	0.000000432811	0.000000432767
t_5	$-0.982438718508 \cdot 10^{-23}$	$-0.981777297429 \cdot 10^{-23}$	$-0.981303186480 \cdot 10^{-23}$	$-0.974860961611 \cdot 10^{-23}$

Table 2: Positions of the local zeros (s_n) and local extrema (r_n), and the values of the local extrema (t_n), for the first eigenfunction of the clamped plate problem (1) for $n = 1$ to 5, as calculated on three different meshes (where N is the number of unknowns in the system (10) for each mesh). The last column contains the corresponding results from [4] where available.

$h \approx rh_1$, and when $h < \rho_1$ the mesh is approximately uniform. In this approach it is necessary to represent the circular arc by a piecewise affine approximation of side length $\approx h_1$. In order to obtain an idea of the magnitude of the errors resulting from such an approximation we choose to perform all calculations on two different polygonal domains: one containing the sector and the other contained by it. It follows from the min-max principle that the m^{th} eigenvalue of the differential operator on the sector is contained between the corresponding eigenvalue on each of these computational domains.

In addition to considering the errors that result from taking an approximation to the domain Ω_θ, it is also desirable to have an indication of the errors associated with approximating the continuous operator by the finite element discretization. In the numerical results that follow the calculations for each different value of θ are presented for two different pairs of meshes of the type described above. Typically, the first pair of such meshes has only about 30% of the number of degrees of freedom as the second. Hence, when intervals for the local zeros/extrema positions obtained on the finer pair of

N	5575	22351	90028
s_1/s_2	16.5671	16.5674	16.5675
s_2/s_3	16.5679	16.5674	16.5674
s_3/s_4	16.5667	16.5674	16.5674
s_4/s_5	16.5663	16.5668	16.5685
limit	16.5674	16.5674	16.5674

Table 3: Ratios between consecutive local zeros as computed on three different meshes (where N is the number of unknowns in the system (10) for each mesh).

	FE method			L–G method [4]
N	5575	22351	90028	5000
r_1/r_2	16.5684	16.5673	16.5674	16.5675
r_2/r_3	16.5727	16.5675	16.5675	16.5674
r_3/r_4	16.5593	16.5677	16.5675	16.5674
r_4/r_5	16.5689	16.5778	16.5784	16.5801
limit	16.5674	16.5674	16.5674	16.5674

Table 4: Ratios between consecutive local extremal positions as computed on three different meshes (where N is the number of unknowns in the system (10) and the system from [4] respectively).

	FE method			L–G method [4]
N	5575	22351	90028	5000
$\|t_1/t_2\|$	36253.4292	36267.6722	36267.6901	36267.7125
$\|t_2/t_3\|$	36272.6177	36267.5198	36267.5223	36267.5498
$\|t_3/t_4\|$	36264.9548	36267.6044	36267.5564	36267.5496
$\|t_4/t_5\|$	36245.7209	36254.0633	36270.7433	36510.3612
limit	36267.5596	36267.5596	36267.5596	36267.5596

Table 5: Ratios between consecutive local extremal values as computed on three different meshes (where N is the number of unknowns in the system (10) and the system from [4] respectively).

meshes are contained within those obtained on the coarser pair, we can have a reasonable expectation of the reliability of these calculations.

Tables 6 and 7 show the computed values of s_n and r_n ($n = 1$ to 4), the positions of the zeros and extrema respectively of the first eigenfunction of (1), for domains Ω_θ with θ between 30° and 140° inclusive.

In each case the numerical results quoted take the form of pairs of values corresponding to those calculated on the inner (bottom value) and outer (top value) polygons respectively. It should be noted that, with one exception, each pair of values in Table 7 lies between the corresponding values in Table 6. While this proves nothing rigorous about bounds on the eigenvalue or the positions of the zeros and the extrema, it does provide a degree of confidence in the calculations. Furthermore, the one value (r_3 when $\theta = 120°$) for which there is any discrepancy between the two sets of results is clearly on the limit of our computational accuracy. Even in this case however, all four estimates of this value agree to two significant figures and have an absolute difference of less than 10^{-9}. The results in Tables 6 and 7 clearly show that, as the theory outlined above predicts, the frequency of the oscillations of the eigenfunction, u, decreases as θ increases. Table 8 further illustrates this point by presenting the ratios of the positions of consecutive zeros and extrema for the fine mesh calculations. This table also shows the known asymptotic limit for these ratios in each case. It is notable that these asymptotic ratios are remarkably well approximated even by the first few ratios that we are able to calculate here. Furthermore, as θ approaches an angle of 140°, it is clear that our numerical calculations are having great difficulty in resolving even the second change of sign. This is to be expected since the solution of equation (4) with smallest real part is equal to $2.826869 + 0.261695i$ for this value of θ: hence, by (5) and (6), the limiting ratio of the position and magnitude of consecutive extrema is equal to 163533.23 and 5.472×10^{14} respectively. Given that r_1 is already very small and

α	$30°$	$40°$	$50°$	$60°$	$70°$	$80°$
h_1	0.065	0.087	0.110	0.132	0.154	0.176
ρ_1	$5 \cdot 10^{-4}$	$5 \cdot 10^{-5}$	$1 \cdot 10^{-6}$	$2.5 \cdot 10^{-7}$	$1 \cdot 10^{-8}$	$1 \cdot 10^{-8}$
N	34009	32980	36655	33421	34450	30040
λ_1	$354^{24.194986}_{43.169162}$	$158^{84.340834}_{99.470006}$	$89^{00.8711417}_{14.1217006}$	$57^{16.2444537}_{28.5030533}$	$40^{21.2855619}_{33.0287132}$	$30^{17.9563370}_{29.4734311}$
s_1	0.3097^{751958}_{337281}	0.2310^{791320}_{241412}	$0.170^{7611453}_{6976522}$	$0.123^{7319839}_{6657365}$	$0.086^{9008096}_{8374821}$	0.0582^{598605}_{044100}
r_1	0.2792^{386428}_{012640}	0.2021^{650011}_{168919}	$0.145^{2199751}_{1659786}$	0.1024^{606481}_{057897}	0.0701^{707180}_{195823}	0.0459^{446784}_{009493}
s_2	0.1459^{854569}_{659148}	0.0835^{949688}_{750755}	$0.046^{5146269}_{4973316}$	0.0247^{433560}_{301082}	0.0123^{245198}_{155385}	0.0055^{829245}_{776108}
r_2	0.1316^{545587}_{369362}	0.0731^{463995}_{289927}	0.0395^{610519}_{463421}	0.0204^{888625}_{778925}	0.0099^{522789}_{450264}	$0.004^{4024756}_{3982853}$
s_3	0.0691^{156363}_{063846}	0.0302^{960386}_{888290}	0.01267^{82277}_{35136}	0.00494^{89459}_{62962}	0.00174^{79807}_{67069}	0.00053^{50025}_{44933}
r_3	0.0623^{300142}_{221671}	0.02650^{83465}_{20383}	0.0107^{832608}_{792514}	0.00409^{81219}_{59277}	0.00141^{14887}_{04601}	0.000421^{9102}_{5086}
s_4	0.03272^{97872}_{54060}	0.0109^{800588}_{77458}	0.00345^{56456}_{43607}	0.000989^{8434}_{3135}	0.000247^{9152}_{7346}	0.0000512^{684}_{196}
r_4	0.02951^{77925}_{38412}	0.00960^{77195}_{54332}	0.00293^{91553}_{80625}	0.000819^{7040}_{2651}	0.000200^{2034}_{0575}	0.000040^{4297}_{3912}

θ	$90°$	$100°$	$110°$	$120°$	$130°$	$140°$
h_1	0.199	0.222	0.245	0.268	0.291	0.315
ρ_1	$1 \cdot 10^{-8}$	$5 \cdot 10^{-9}$	$2.5 \cdot 10^{-9}$	$5 \cdot 10^{-10}$	$5 \cdot 10^{-10}$	$5 \cdot 10^{-10}$
N	29746	24601	23092	22651	20887	19270
λ_1	$23^{76.3155992}_{87.7996658}$	$19^{41.3070303}_{52.8971428}$	$16^{32.6947173}_{44.4979497}$	$14^{05.7227746}_{17.8265343}$	$12^{33.8788513}_{46.3582958}$	$11^{00.6652772}_{13.5880500}$
s_1	0.0364^{463359}_{024346}	0.0204^{920930}_{616208}	0.0096^{573740}_{399984}	0.0032^{737930}_{667832}	0.00051^{41408}_{28490}	0.0000035^{415}_{312}
r_1	$0.028^{1063243}_{0724689}$	0.0154^{743684}_{513578}	0.0071^{498633}_{369993}	0.00237^{92947}_{42004}	0.00036^{72098}_{62871}	0.0000024^{88}_{15}
s_2	0.00219^{98778}_{72279}	$0.000^{7000095}_{6989686}$	0.000156^{5374}_{2557}	0.000018^{1274}_{0886}	0.00000045^{12}_{01}	—
r_2	0.00169^{65096}_{44661}	0.00052^{86069}_{78278}	0.000115^{8947}_{6862}	0.0000131^{743}_{461}	0.00000032^{23}_{15}	—
s_3	0.000132^{7834}_{6235}	0.000023^{9123}_{8767}	0.0000025^{73}_{28}	0.000000100^{4}_{2}	—	—
r_3	0.000102^{4022}_{2789}	0.0000180^{567}_{306}	0.0000018^{86}_{52}	0.000000072^{9}_{8}	—	—
s_4	0.0000080^{147}_{051}	0.0000008^{68}_{56}	0.000000041^{1}_{0}	—	—	—
r_4	0.0000061^{810}_{736}	0.00000061^{68}_{59}	0.000000030^{5}_{4}	—	—	—

Table 6: Local zeros (s_n) and local extrema (r_n), as calculated on the coarse meshes, of the first eigenvalue for the clamped plate eigenvalue problem on a circular sector of angle θ.

$|t_1| \approx 1.30729 \cdot 10^{-15}$ times the maximum magnitude of u, double precision calculations could not reasonably be expected to locate the second extremum with any significant figures of accuracy. For this reason, in Table 9 we are only able to present calculations of the location of the first zero of u when considering values of θ greater than $140°$. The parameters used for the generation of the meshes for these calculations are $\rho_1 = 5 \cdot 10^{-10}$ and $h_1 \approx 0.16$, which, in principal at least, allow us to observe a sign change at a distance of $O(10^{-11})$ from the corner. In practice however we are unable to detect the first change in sign when $\theta = 145°$ and $\theta = 146°$ using such meshes. Nevertheless it is clear that these simple calculations do verify the theory which predicts the loss of oscillations at some critical angle θ_c, even though we are unable to accurately determine a value for θ_c using these meshes.

Another interesting situation to investigate numerically would be the limiting behaviour of the principal eigenfunction as $\theta \to 0$. Theory predicts that, as θ decreases, oscillations will become more frequent and their amplitude will decay more quickly as a function of r (although the asymptotic ratio of successive eigenvalues will decrease). This presents different, but equally demanding, computational challenges to those for $\theta \to \theta_c$. In particular it is no longer sufficient to refine the mesh heavily only in the neighbourhood of the corner since changes in sign occur frequently throughout a

α	$30°$	$40°$	$50°$	$60°$	$70°$	$80°$
h_1	0.033	0.044	0.055	0.066	0.077	0.087
ρ_1	$1 \cdot 10^{-2}$	$2 \cdot 10^{-3}$	$2.5 \cdot 10^{-4}$	$5 \cdot 10^{-5}$	$1 \cdot 10^{-5}$	$1 \cdot 10^{-6}$
N	82084	82627	87865	87283	86701	90775
λ_1	$354^{28.863922}_{33.606980}$	$158^{88.056086}_{91.837688}$	$890^{4.1158527}_{7.4275436}$	$57^{19.2365745}_{22.2999555}$	$402^{4.1419602}_{7.0760866}$	$302^{0.7476335}_{3.6247696}$
s_1	0.3097^{650827}_{547154}	0.2310^{656892}_{519414}	0.1707^{452024}_{293299}	$0.123^{7158333}_{6992733}$	0.0868^{852561}_{694257}	0.0582^{464922}_{326311}
r_1	0.2792^{356059}_{262612}	0.2021^{466898}_{346638}	$0.145^{2116893}_{1981906}$	0.1024^{451849}_{314713}	0.0701^{601000}_{473169}	0.0459^{331081}_{221772}
s_2	0.1459^{806409}_{757551}	0.08358^{99082}_{49350}	0.0465^{102813}_{059576}	0.0247^{400416}_{367298}	0.01232^{23226}_{00774}	0.0055^{801286}_{792134}
r_2	0.13164^{89477}_{45423}	0.0731^{414045}_{370529}	0.03955^{75761}_{38988}	0.02048^{69531}_{42106}	0.0099^{503538}_{485408}	0.00440^{16326}_{05850}
s_3	0.06911^{32761}_{09631}	0.03029^{42219}_{24195}	0.01267^{70587}_{58803}	0.00494^{82884}_{76260}	0.001747^{6664}_{3480}	0.000534^{8774}_{7501}
r_3	0.06232^{90547}_{69688}	0.02650^{76150}_{60380}	0.01078^{20009}_{09985}	0.004097^{5905}_{0420}	0.00141^{12570}_{09998}	0.000421^{8016}_{7013}
s_4	0.03272^{88491}_{77538}	0.01097^{94226}_{87694}	0.003455^{3299}_{0087}	0.000989^{7136}_{5811}	0.0002478^{703}_{252}	0.0000512^{564}_{442}
r_4	0.02951^{62568}_{52608}	0.00960^{70576}_{64861}	0.002938^{8023}_{5291}	0.000819^{5669}_{4572}	0.0002001^{584}_{219}	0.0000404^{206}_{110}

θ	$90°$	$100°$	$110°$	$120°$	$130°$	$140°$
h_1	0.098	0.110	0.121	0.132	0.143	0.154
ρ_1	$2.5 \cdot 10^{-7}$	$5 \cdot 10^{-8}$	$1 \cdot 10^{-8}$	$2.5 \cdot 10^{-9}$	$5 \cdot 10^{-10}$	$5 \cdot 10^{-10}$
N	88447	87865	87283	85828	85246	79096
λ_1	$23^{79.0885238}_{81.9568311}$	$194^{4.0948765}_{6.9890139}$	$163^{5.5227545}_{8.4693656}$	$14^{08.6112832}_{11.6320780}$	$123^{6.8449411}_{9.9585482}$	$110^{3.7240407}_{6.9471887}$
s_1	0.0364^{357449}_{247712}	0.0204^{846824}_{770656}	0.0096^{532030}_{488600}	0.00327^{21026}_{03507}	0.000513^{8318}_{5089}	0.0000353^{91}_{65}
r_1	0.02809^{86552}_{01923}	0.01546^{87697}_{30180}	0.00714^{68898}_{36744}	0.00237^{80040}_{67308}	0.000366^{9966}_{7660}	0.0000248^{71}_{53}
s_2	0.00219^{92365}_{85741}	0.000699^{7556}_{4954}	0.000156^{4694}_{3990}	0.0000181^{180}_{083}	0.000000450^{9}_{7}	—
r_2	0.00169^{60167}_{55059}	0.000528^{4129}_{2165}	0.000115^{8435}_{7914}	0.00001316^{74}_{03}	0.00000032^{21}_{19}	—
s_3	0.0001327^{446}_{046}	0.000023^{9036}_{8947}	$0.0000025 3^{62}_{51}$	0.000000100^{3}_{2}	—	—
r_3	0.0001023^{699}_{391}	0.0000180^{506}_{439}	$0.0000018 7^{73}_{69}$	$0.0000000 7^{30}_{29}$	—	—
s_4	0.00000801^{24}_{00}	0.000000816^{5}_{2}	0.0000000411	—	—	—
r_4	0.00000617^{90}_{71}	0.000000616^{5}_{4}	0.0000000304	—	—	—

Table 7: Local zeros (s_n) and local extrema (r_n), as calculated on the fine meshes, of the first eigenvalue for the clamped plate eigenvalue problem on a circular sector of angle θ.

large part of the domain. Hence, for very small angles θ, a very dense finite element mesh is required over almost all of Ω_θ which, despite the narrowing of the domain, leads to very large algebraic systems (10). In fact, even for $\theta = 10°$, we observe a reduction in the apparent rate of convergence when considering the position of the zeros of u on sequences of finer meshes. This leads us to believe that a thorough numerical investigation of the behaviour of this eigenfunction as $\theta \to 0$ will be an even more computationally demanding task.

In the numerical results that we present above it has been possible, for the first time that we are aware, to verify a number of theoretical asymptotic results concerning the existence of nodal lines in the vicinity of a corner with arbitrary internal angle θ. Furthermore we have computed, with some confidence, estimates for the exact locations of zeros and extrema of the principal eigenfunction for a number of different values of θ. More comprehensive results, including those for the buckling plate problem, (2), can also be found in [19]. In the following section we move on from providing numerical verification and extensions of known analytic results to demonstrate that numerics can also give some insight into problems for which there are no theoretical predictions.

θ	30°	40°	50°	60°	70°	80°
s_1/s_2	2.1219600	2.7642773	3.6711281	5.0006316	7.0510454	10.435415
s_2/s_3	2.1121939	2.7592690	3.6688543	4.9997170	7.0507290	10.435321
s_3/s_4	2.1116928	2.7591817	3.6688418	4.9997176	7.0507283	10.435323
limit	2.1116888	2.7591817	3.6688419	4.9997171	7.0507288	10.435321
r_1/r_2	2.1210622	2.7637792	3.6708945	5.0005086	7.0510156	10.435471
r_2/r_3	2.1121602	2.7592601	3.6688530	4.9997561	7.0507030	10.435314
r_3/r_4	2.11168^{56}_{62}	2.7591814	3.6688418	4.9997024	7.0507288	10.435311
limit	2.1116888	2.7591817	3.6688419	4.9997171	7.0507288	10.435321

θ	90°	100°	110°	120°	130°	140°
s_1/s_2	16.567452	29.274052	61.693788	180.59907	1139.4^{505}_{724}	—
s_2/s_3	16.567430	29.274040	61.693978	180.5^{8995}_{9586}	—	—
s_3/s_4	16.567425	29.274^{355}_{153}	$61.^{718979}_{673203}$	—	—	—
limit	16.56743	29.27404	61.69387	180.5992	1139.464	163533.2
r_1/r_2	16.567440	29.274017	61.694352	180.598^{28}_{34}	1139.4^{312}_{450}	—
r_2/r_3	16.567535	29.27394^{8}_{0}	61.693^{540}_{744}	180.62^{481}_{716}	—	—
r_3/r_4	16.5674^{17}_{25}	29.274^{727}_{105}	61.7^{30719}_{51464}	—	—	—
limit	16.56743	29.27404	61.69387	180.5992	1139.464	163533.2

Table 8: Ratios of consecutive local zeros and extrema of the eigenfunction (along with the theoretical asymptotic value) for different values of θ.

θ	141°	142°	143°	144°	145°	146°	147°
s_1	0.00000111^{248}_{165}	0.000000240^{66}_{47}	0.0000000275^{1}_{0}	0.000000000^{93}_{85}	—	—	—

Table 9: Calculated positions of the local zeros of the eigenfunction for values of θ above 140°.

4 Parity property of eigenfunctions

In this section we again consider problems (1) and (2) but now on another family of domains, Ω_c say, which are defined as the regions bounded by the curves (7) for $c > 0$. We are particularly interested in the behaviour of the eigenfunctions which correspond to the smallest eigenvalues as $c \to 0$. In this limit the connected domain Ω_c tends to a disconnected domain which is symmetric about the $y-$axis. It follows therefore that each eigenvalue must have an even multiplicity and, in particular, the smallest eigenvalue will be repeated. When $c > 0$, but small, therefore, we expect the eigenvalues of the biharmonic operator to occur in distinct pairs (i.e. there will be a small gap between the $(2k-1)^{th}$ and the $2k^{th}$ eigenvalues for positive integers k). The same argument holds when considering the *Laplacian* eigenvalue problem on Ω_c, subject to zero Dirichlet boundary conditions. Indeed, it is known that for this second order problem the eigenfunction corresponding to the lower eigenvalue in each pair is always an even function of x while the other eigenfunction in the pair is always odd. No such result is known in the case of the biharmonic operator however. In Table 10 below we present numerical evidence that such a result is false. This is achieved by demonstrating that branches of the two least eigenvalues (corresponding to eigenfunctions of different parity), viewed as functions of c, appear to cross on more than one occasion as c approaches zero.

c	$\lambda_{even}/\lambda_{odd}$	λ_{even}	λ_{odd}	N
1.0	0.304005	51.9393395	170.850197	129602
0.9	0.349358	68.2814038	195.448422	141122
0.8	0.410835	94.5437752	230.125842	152642
0.7	0.494593	139.440088	281.928749	108290
0.6	0.608020	221.940406	365.021620	119810
0.5	0.755019	385.377821	510.421666	133634
0.4	0.914099	724.064578	792.107738	112754
0.35	0.972477	1005.87754	1034.34630	120530
0.325	0.990509	1185.48005	1196.83874	128306
0.3	1.000849	1397.46767	1396.29291	134138
0.275	1.004906	1650.06652	1642.01017	141914
0.25	1.004943	1955.47056	1945.85190	151634
0.225	1.003236	2330.95499	2323.43715	161354
0.2	1.001465	2800.48607	2796.38901	136514
0.175	1.000403	3396.70646	3395.33941	125138
0.15	1.000031	4165.22544	4165.09438	136226
0.125	0.999987	5172.36322	5172.42820	152066
0.1	0.999998	6518.06051	6518.07172	144002
0.075	1.000000	8356.71703	8356.71678	136082
0.05	1.000000	10936.0178	10936.0178	133634
0.025	1.000000	14670.7338	14670.7338	126362
0.01	1.000000	17752.3432	17752.3432	118082

Table 10: Estimates of the two smallest eigenvalues, and their parity, for the clamped plate problem on Ω_c.

The results presented have been calculated using the same piecewise cubic mixed finite element method described and used in the previous sections. In practice our computations were performed on a discretization of Ω_c in which the curved boundary is represented by an interpolating polygon. Since our motivation here is primarily to find an example in which the parity of the eigenfunctions changes with the domain geometry, this approximation is of no significant consequence. We again make use of unstructured meshes of triangles in the interior of the domain and use N to represent the total number of degrees of freedom in the finite element approximation. For each value of c calculations were performed on a sequence of meshes with different numbers of triangles. Only the results of computations on the finest meshes are presented in Table 10, however an indication of the reliability of these figures is given by comparison with the corresponding calculations on coarser meshes. In particular, Table 11 gives the relative differences (as percentages) between consecutive ratios $\lambda_{even}/\lambda_{odd}$ computed on four different meshes for each value of the parameter c. In the table N_i $(i = 1, \dots, 4)$ denotes the total dimension of the linear system arising from the four different discretizations of the domain, and $\delta\,(\%)$ stands for the relative difference in the ratios $\lambda_{even}/\lambda_{odd}$ computed on consecutive meshes. It is reasonable to expect that our results are reliable if this relative "error" decreases (and becomes sufficiently small) as the mesh is refined. As we can see from Table 11 this is the case for all meshes and all values of the parameter c considered.

Table 10 clearly shows that, for our finite element discretization at least, there are indeed values of c for which the branches of the two smallest eigenvalues cross. Inspection of the corresponding

c	1.0	0.9	0.8	0.7	0.6	0.5	0.4	0.35	0.325	0.3	0.275
N_1	52202	54002	59402	41762	47522	53282	50546	54434	57026	60914	63506
N_2	73442	79922	86402	60482	67394	76034	68042	74090	78626	81650	86186
$\delta\,(\%)$	1.18e-2	1.46e-2	1.29e-2	1.97e-2	1.45e-2	1.21e-2	6.15e-3	3.24e-3	1.75e-3	7.70e-4	2.47e-4
N_2	73442	79922	86402	60482	67394	76034	68042	74090	78626	81650	86186
N_3	98282	105842	115922	80642	90722	102818	89858	95042	101954	105410	112322
$\delta\,(\%)$	7.47e-3	6.81e-3	7.77e-3	9.19e-3	8.95e-3	6.14e-3	4.84e-3	1.79e-3	1.16e-3	5.19e-4	1.38e-4
N_3	98282	105842	115922	80642	90722	102818	89858	95042	101954	105410	112322
N_4	129602	141122	152642	108290	119810	133634	112754	120530	128306	134138	141914
$\delta\,(\%)$	5.03e-3	5.89e-3	5.05e-3	7.93e-3	5.90e-3	5.01e-3	2.69e-3	1.53e-3	8.05e-4	4.19e-4	1.16e-4

c	0.25	0.225	0.2	0.175	0.15	0.125	0.1	0.075	0.05	0.025	0.01
N_1	68690	72758	76466	66818	73730	80642	70562	82658	52562	74882	58466
N_2	92234	96770	95042	84242	93314	102386	92162	108290	75170	91082	76034
$\delta\,(\%)$	3.02e-5	8.81e-5	4.88e-5	2.42e-5	4.80e-6	9.99e-8	9.99e-8	0.000	0.000	0.000	0.000
N_2	92234	96770	95042	84242	93314	102386	92162	108290	75170	91082	76034
N_3	119234	127874	115634	103682	112322	126722	116642	122402	101810	108002	95906
$\delta\,(\%)$	2.01e-5	6.43e-5	3.64e-5	1.79e-5	3.10e-6	9.99e-8	9.99e-8	0.000	0.000	0.000	0.000
N_3	119234	127874	115634	103682	112322	126722	116642	122402	101810	108002	95906
N_4	151634	161354	136514	125138	136226	152066	144002	136082	133634	126362	118082
$\delta\,(\%)$	1.41e-5	4.42e-5	2.78e-5	1.50e-5	2.60e-6	0.000	0.000	0.000	0.000	0.000	0.000

Table 11: Percentage discrepancies δ between the ratios $\lambda_{even}/\lambda_{odd}$ obtained on four different meshes for each domain Ω_c (discrepancies of less than 1.0e-8 have been rounded to zero).

eigenfunctions demonstrates that one of these functions is always even and the other is always odd: we refer to the associated eigenvalues as $\lambda_{even}(c)$ and $\lambda_{odd}(c)$ respectively. Further numerical computations on a sequence of coarser grids, [19], suggest that as the mesh size h is reduced, the locations of these crossing points remain stable and the difference between $\lambda_{even}(c)$ and $\lambda_{odd}(c)$ does not tend to zero for values of c between these points. This suggests that it is reasonably safe for us to conclude that the parity of the eigenfunction corresponding to the least eigenvalue of (1) does indeed change as the domain Ω_c evolves. Although we have only presented results for the clamped plate problem here, it is shown in [19] that similar behaviour may be observed for the buckling plate problem (2) on these domains. It is interesting to hypothesize on the behaviour of the eigenvalue branches as c gets very close to its limiting value of zero. The resolution of the computations that we have undertaken only appears to allow us to identify the first two or three values of c for which the least eigenvalue is repeated. Beyond this point discretization and rounding errors make it impossible to distinguish between them, even though they are almost certainly different for most values of $c > 0$. There may however be further values of c, smaller than those that we have been able to identify, for which $\lambda_{even}(c) = \lambda_{odd}(c)$: we conjecture that there are an infinite number of such values.

5 Discussion

In this paper our aim has been to demonstrate that the finite element method may be successfully applied to biharmonic eigenvalue problems of the form (1) and (2), and that it may be used both to verify existing asymptotic results and to allow new conjectures to be made about the behaviour of their eigenfunctions. An outline of the finite element implementation is given in Section 2, with complete details available in [8]. Verification of the accuracy of this approach is provided by comparison with known analytical results applied on a unit square domain, along with the recent high precision numerical results (calculated using an entirely different discretization scheme) that appear in [4].

An advantage of the mixed finite element method used in this work is that it may easily be applied on unstructured grids of triangles, $\mathcal{T}^h$, and therefore on arbitrary polygonal domains in $\Re^2$. We have made use of this fact to investigate the spectral properties of the biharmonic operator on two further geometries: sectors of the unit circle and a family of non-convex domains. Furthermore it is possible to generate meshes for which the degrees of freedom in the corresponding piecewise cubic trial spaces are not uniformly distributed throughout Ω. Where appropriate, this allows us to obtain a greater resolution of the eigenfunctions in those regions in which we wish to focus, without affecting either the dimension or the sparsity of the discrete linear system (10).

The results presented in Section 3 are in agreement with the asymptotic theory that appears in [6],[12],[17],[18] and also provide quantitative estimates of the positions of a number of sign changes and extremal points for various values of the internal angle θ. In Section 4 we extend the numerical investigation further by considering a family of problems for which the eigenfunctions have significantly different qualitative properties. This has led to evidence that, unlike the Laplace operator, the parity of the least eigenfunction of the biharmonic operator can change as the domain is deformed.

The unstructured finite element approach that we have used in this work may also be applied to further problems in this area. Clearly it is possible to investigate the spectral properties of the biharmonic operator on a greater variety of geometries in 2-d, and subject to a wider variety of boundary conditions. This would include, for example, further studies in the circular sector domains for very small angles θ. Perhaps more interestingly however (and certainly more computationally demanding) would be extensions to higher order operators and/or larger numbers of dimensions.

We conclude this paper by noting that none of the computational results that are presented here provide *rigorous* information about the eigenfunctions considered (although the apparent mesh convergence observed is certainly a strong indicator). It would be interesting therefore to attempt to obtain provably correct bounds for certain quantities associated with the eigenvalues and eigenfunctions of the biharmonic operator on the regions considered. In [24], for example, Weiners has made a start on this problem by computing enclosures for the first eigenfunction in the neighbourhood of a corner of the unit square. This involves computing estimates for the Sobolev embedding constants which in turn requires an upper bound for the defect of the eigenfunction. He is able to show that the defect is less than 0.000000893 which is sufficiently accurate to allow him to conclude that the first eigenfunction changes sign. Since the estimates of the amplitude of the second and higher sign changes that we have found are considerably smaller than for the first, new methods are likely to be required in order to compute the defect with sufficient precision.

Acknowledgements

BMB and MDM acknowledge the EPRSC for support under grant GR/K84745 and PKJ acknowledges the support of the Leverhulme Trust.

References

[1] L. Bauer, E. Reiss: *Block five diagonal matrices and the fast numerical computation of the biharmonic equation,* Math. Comp., **26**(1972), 311–326.

[2] H. Behnke: *A numerically rigorous proof of curve veering for a plate,* Second Gregynog Workshop on Computational and Analytic Problems in Spectral Theory, Cardiff University, 1996.

[3] P.E. BjøRstad, B.P. Tjøstheim: *Efficient algorithms for solving a fourth order equation with the spectral Galerkin method,* SIAM J. Sci. Comp., **18**(2)(1997), 621–632.

[4] P.E. Bjørstad, B.P. Tjøstheim: *A note on high precision solutions of two fourth order eigenvalue problems,* preprint, 1998.

[5] P.E. BjøRstad, B.P. Tjøstheim: *Private communication.*

[6] H. Blum, R. Rannacher: *On the boundary value problem of the biharmonic operator on domains with angular corners,* Math. Meth. in Appl. Sci., **2**(1980), 556–581.

[7] F. Brezzi: *On the existence, uniqueness and approximation of saddle point problems arising from Lagrangian multipliers,* RAIRO, **8**(1974), 129–151.

[8] B.M. Brown, P.K. Jimack, M.D. Mihajlović: *An efficient direct solver for a class of mixed finite element problems,* School of Computer Studies Research Report 99.03, University of Leeds, 1999 (submitted to Applied Numerical Mathematics).

[9] G. Chen, M. Coleman, J. Zhou: *Analysis of vibration eigenfrequencies of a thin plate by the Keller–Rubinow wave method I: clamped boundary conditions with rectangular or circular geometry,* SIAM J. Appl. Math., **51**(1991), 967–983.

[10] P.G. Ciarlet: *The Finite Element Method for Elliptic Problems,* Stud. Math. Appl., 4, North–Holland, Amsterdam, 1978.

[11] P.G. Ciarlet, P. Raviart: *A mixed finite element method for the biharmonic equation,* In: Mathematical Aspects of Finite Elements in Partial Differential Equations, Academic Press, New York, 1974, pp. 125–145.

[12] C.V. Coffman: *On the structure of solutions $\Delta^2 u = \lambda u$ which satisfy the clamped plate conditions on a right angle,* SIAM J. Math. Anal., **13**(1982), 746–757.

[13] E.B. Davies: *Spectral Theory and Differential Operators,* Cambridge Univ. Press, Cambridge, 1995.

[14] E.B. Davies: *L^p spectral theory of higher-order elliptic differential operators,* Bull. London Math. Soc., **29**(1997), 513–546.

[15] G.H. Golub, C.F. Van Loan: *Matrix Computations,* Second Edition, The John Hopkins University Press, Baltimore, 1989.

[16] W. Hackbusch, G. Hoffman: *Results of the eigenvalue problem for the plate equation,* ZAMP, **31**(1980), 730–739.

[17] V.A. Kondrat'ev: *Boundary problems for elliptic equations in domains with conical or angular points,* Trans. Moscow Math. Soc., **16**(1967), 227–313.

[18] V.A. Kozlov, V.A. Kondrat'ev, V.G. Maz'ya: *On sign variation and the absence of "strong" zeros of solutions of elliptic equations,* Mat. USSR Izv., **34**(1990), 337–353.

[19] M.D. Mihajlović: *A numerical investigation of some problems associated with the biharmonic operator,* Ph.D. Thesis, Department of Computer Science, Cardiff University, 1999.

[20] V.V. Shaidurov: *Multigrid Methods for Finite Elements,* Kluwer, Dodrecht, 1995.

[21] G. Strang, G.J. Fix: *An Analysis of the Finite Element Method,* Prentice-Hall, Englewood-Cliffs, 1973.

[22] J. Shen: *Efficient spectral Galerkin method I: direct solvers of second and fourth order equations using Legendre polynomials,* SIAM J. Sci. Comput., **15**(1994), 1440–1451.

[23] S. Timoshenko, S. Woinowsky–Krieger: *Theory of plates and shells,* McGraw-Hill, New York, 1959.

[24] C. Wieners: *A numerical existence proof of nodal lines for the first eigenfunction of the plate equation,* Arch. Math., **66**(1996), 420–427.

[25] O.C. Zienkiewicz: *The Finite Element Method,* Third edition, McGraw-Hill, London, 1986.